AIMS Mathematics

http://www.aimspress.com/journal/Math

AIMS Mathematics, 8(1): 1230–1250.
DOI:10.3934/math.2023062
Received: 21 July 2022
Revised: 14 September 2022
Accepted: 23 September 2022
Published: 18 October 2022

Research article

Traveling-wave and numerical solutions to a Novikov-Veselov system via the modified mathematical methods

Abdulghani R. Alharbi*

Department of Mathematics, College of Science, Taibah University, Al-Madinah Al-Munawarah, Saudi Arabia

* **Correspondence:** E-mail: arharbi@taibahu.edu.sa, abdul928@hotmail.com.

Abstract: In this article, we have achieved new solutions for the Novikov-Veselov system using several methods. The present solutions contain soliton solutions in the shape of hyperbolic, rational, and trigonometric function solutions. Magneto-sound and ion waves in plasma are examined by employing partial differential equations, such as, the Novikov-Veselov system. The Generalized Algebraic and the Modified F-expansion methods are employed to achieve various soliton solutions for the system. The finite difference method is well applied to convert the proposed system into numerical schemes. They are used to obtain the numerical simulations for NV. I also present a study of the stability and Error analysis of the numerical schemes. To verify the validity and accuracy of the exact solutions obtained using exact methods, we compare them with the numerical solutions analytically and graphically. The presented methods in this paper are suitable and acceptable and can be utilized for solving other types of non-linear evolution systems.

Keywords: Novikov-Veselov equations; solitary solutions; numerical solutions; magnetosound; electromagnetic
Mathematics Subject Classification: 35A24, 35B35, 35Q51, 35Q92, 65N06, 65N40, 65N45, 65N50

1. Introduction

In various fields of science, nonlinear evolution equations practically model many natural, biological and engineering processes. For example, PDEs are very popular and are used in physics to study traveling wave solutions. They have played a crucial role in illustrating the nature of nonlinear problems. PDEs are collected to control the diffusion of chemical reactions. In biology, they play a fundamental role in describing various phenomena, such as population growth. In addition, natural phenomena such as fluid dynamics, plasma physics, optics and optical fibers, electromagnetism, quantum mechanics, ocean waves, and others are studied using PDEs. The qualitative and quantitative characteristics of these phenomena can be identified from the behaviors and shapes of their solutions. Therefore, finding the analytic solutions to such phenomena is a fundamental topic in mathematics. Scientists have developed sparse fundamental approaches to find analytic solutions for nonlinear PDEs. Among these techniques, I present integration methods from [1] and [2], the modified F-expansion and Generalized Algebraic methods, respectively. Bekir and Unsal [3] proposed the first integral method to find the analytical solution of nonlinear equations. Kumar, Seadawy and Joardar [4] used the improved Kudryashov technique to extract fractional differential equations. Adomian [5] proposed the Adomian decomposition technique to find the solution of frontier problems of physics. [6] uses an exploratory method to find explicit solutions of non-linear PDEs. Many different methods of solving equations arising from natural phenomena and some of their analytic solutions, such as dark and light solitons, non-local rogue waves, an occasional wave and mixed soliton solutions, are exhibited and can be found in [7–40].

The Novikov-Veselov (NV) system [41, 42] is given by

$$\begin{aligned} &\Psi_t + \alpha\Gamma_{xxy} + \beta\Phi_{xyy} + \gamma\Gamma_y\Phi + \gamma\left(\frac{\Psi^2}{2}\right)_y + \lambda\,\Gamma\,\Phi_x + \lambda\left(\frac{\Psi^2}{2}\right)_x = 0,\\ &\Gamma_y = \Psi_x,\\ &\Psi_y = \Phi_x, \end{aligned} \tag{1.1}$$

where α, β, γ and λ are constants. Barman [42] declared that Eq (1.1) is involved to represent tidal and tsunami waves, electro-magnetic waves in communication cables and magneto-sound and ion waves in plasma. In [42], the generalized Kudryashov method was utilized to have traveling wave solutions for Eq (1.1). According to Croke [43], the Novikov-Veselov system is generalized from the KdV equations which were examined by Novikov and Veselov. Croke [43] used several approaches, (the extended mapping, the Hirota and the extended tanh-function approaches) in the proposed system to achieve numerous soliton solutions, such as breathers, and constrained analytic solutions. Boiti, Leon, and Manna [44] applied the inverse dispersion technique to solve (1.1) for a particular type of initial value. Numerical solutions and a study of the stability of solutions for the proposed equation were presented by Kazeykina and Klein [45]. The Nizhnik-Novikov-Veselov system for two dimensions was also solved using the Kansa technique to find the numerical results [46]. To the best of my knowledge, the stability and error analysis of the numerical scheme presented here has not yet been discussed for system (1.1). Therefore, this has motivated me enormously to do so. The primary purpose is to obtain multiple analytic solutions to system (1.1) by using both the modified F-expansion and Generalized Algebraic methods. In connection with the numerical solution, the method of finite differences is utilized to achieve numerical results for the studied system. I graphically and analytically compare the traveling wave solutions and numerical results. Undoubtedly, the presented results strongly contribute to describing physical problems in practice.

The outline of this article is provided in this paragraph. Section 2 summarizes the employed methods. All the analytic solutions are extracted in Section 3. The shooting and BVP results for the proposed system are presented in Section 4. In addition, I examine the numerical solution of the system (1.1) in Section 5. Sections 6 and 7 study the stability and error analysis of the numerical scheme, respectively. Section 8 presents the results and discussion.

2. Summary of proposed methods

Considering the development equation with physical fields $\Psi(x,y,t)$, $\Phi(x,y,t)$ and $\Gamma(x,y,t)$ in the variables x, y and t is given in the following form:

$$Q_1(\Psi, \Psi_t, \Psi_x, \Psi_y, \Gamma, \Gamma_y, \Gamma_{xxy}, \Phi, \Phi_{xyy}, \Phi_x, \dots) = 0. \tag{2.1}$$

Step 1. We extract the traveling-wave solutions of System (1.1) that are formed as follows:

$$\begin{aligned} \Phi(x,y,t) &= \phi(\eta), \qquad\qquad \eta = x + y - wt,\\ \Psi(x,y,t) &= \psi(\eta),\\ \Gamma(x,y,t) &= \Theta(\eta), \end{aligned} \tag{2.2}$$

where w is the wave speed.
Step 2. The nonlinear evolution (2.1) is reduced to the following ODE:

$$Q_2(\psi, \psi_\eta, \Theta, \Theta_\eta, \Theta_{\eta\eta\eta}, \phi, \phi_{\eta\eta\eta}, \phi_\eta, \dots) = 0, \tag{2.3}$$

where Q_2 is a polynomial in $\psi(\eta)$, $\phi(\eta)$, $\Theta(\eta)$ and their total derivatives.

2.1. The modified F-expansion method

According to the modified F-expansion method, the solutions of (2.3) are given by the form

$$\psi(\eta) = \rho_0 + \sum_{k=1}^{N}\left(\rho_k F(\eta)^k + \frac{q_k}{F(\eta)^k}\right), \tag{2.4}$$

and $F(\eta)$ is a solution of the following differential equation:

$$F'(\eta) = \mu_0 + \mu_1 F(\eta) + \mu_2 F(\eta)^2, \tag{2.5}$$

where μ_0, μ_1, μ_2, are given in Table 1 [1], and ρ_k, q_k are to be determined later.

Table 1. The relations among μ_0, μ_1, μ_2 and the function $F(\eta)$.

μ_0	μ_1	μ_2	$F(\eta)$
$\mu_0 = 0$,	$\mu_1 = 1$,	$\mu_2 = -1$,	$F(\eta) = \frac{1}{2} + \frac{1}{2}\tanh\left(\frac{1}{2}\eta\right)$.
$\mu_0 = 0$,	$\mu_1 = -1$,	$\mu_2 = 1$,	$F(\eta) = \frac{1}{2} - \frac{1}{2}\coth\left(\frac{1}{2}\eta\right)$.
$\mu_0 = \frac{1}{2}$,	$\mu_1 = 0$,	$\mu_2 = \frac{-1}{2}$,	$F(\eta) = \coth(\eta) \pm \mathrm{csch}(\eta)$, $\tanh(\eta) \pm \mathrm{sech}(\eta)$.
$\mu_0 = 1$,	$\mu_1 = 0$,	$\mu_2 = -1$,	$F(\eta) = \tanh(\eta)$, $\coth(\eta)$.
$\mu_0 = \frac{1}{2}$,	$\mu_1 = 0$,	$\mu_2 = \frac{1}{2}$,	$F(\eta) = \sec(\eta) + \tan(\eta)$, $\csc(\eta) - \cot(\eta)$.
$\mu_0 = \frac{1}{2}$,	$\mu_1 = 0$,	$\mu_2 = \frac{1}{2}$,	$F(\eta) = \sec(\eta) - \tan(\eta)$, $\csc(\eta) + \cot(\eta)$.
$\mu_0 = \pm 1$,	$\mu_1 = 0$,	$\mu_2 = \pm 1$,	$F(\eta) = \tan(\eta)$, $\cot(\eta)$.

2.2. The generalized algebraic method

According to the generalized direct algebraic method, the solutions of (2.3) are given by

$$\psi(\eta) = \nu_0 + \sum_{k=1}^{N}\left(\nu_k G(\eta)^k + \frac{r_k}{G(\eta)^k}\right), \tag{2.6}$$

and $G(\eta)$ is a solution of the following differential equation:

$$G'(\eta) = \varepsilon\sqrt{\sum_{k=0}^{4}\delta_k G^k(\eta)}, \tag{2.7}$$

where ν_k, and r_k are to be determined, and N is an integer number obtained by the highest degree of the nonlinear terms and the highest order of the derivatives. ε is user-specified, usually taken with $\varepsilon = \pm 1$, and δ_k, $k = 0, 1, 2, 3, 4$, are given in Table 2 [2].

Table 2. The relations among δ_k, $k = 0, 1, 2, 3, 4$, and the function $G(\eta)$.

δ_0	δ_1	δ_2	δ_3	δ_4	$G(\eta)$
$\delta_0 = 0,$	$\delta_1 = 0,$	$\delta_2 > 0,$	$\delta_3 = 0,$	$\delta_4 < 0,$	$G(\eta) = \varepsilon\sqrt{-\frac{\delta_2}{\delta_4}}\,\mathrm{sech}\left(\sqrt{\delta_2}\eta\right).$
$\delta_0 = \frac{\delta_2^2}{4c4},$	$\delta_1 = 0,$	$\delta_2 < 0,$	$\delta_3 = 0,$	$\delta_4 > 0,$	$G(\eta) = \varepsilon\sqrt{-\frac{\delta_2}{2\delta_4}}\tanh\left(\sqrt{-\frac{\delta_2}{2}}\eta\right).$
$\delta_0 = 0,$	$\delta_1 = 0,$	$\delta_2 < 0,$	$\delta_3 = 0,$	$\delta_4 > 0,$	$G(\eta) = \varepsilon\sqrt{-\frac{\delta_2}{\delta_4}}\sec\left(\sqrt{-\delta_2}\eta\right).$
$\delta_0 = \frac{\delta_2^2}{4\delta_4},$	$\delta_1 = 0,$	$\delta_2 > 0,$	$\delta_3 = 0,$	$\delta_4 > 0,$	$G(\eta) = \varepsilon\sqrt{\frac{\delta_2}{2\delta_4}}\tan\left(\sqrt{\frac{\delta_2}{2}}\eta\right).$
$\delta_0 = 0,$	$\delta_1 = 0,$	$\delta_2 = 0,$	$\delta_3 = 0,$	$\delta_4 > 0,$	$G(\eta) = -\frac{\varepsilon}{\sqrt{\delta_4}\eta}.$
$\delta_0 = 0,$	$\delta_1 = 0,$	$\delta_2 > 0,$	$\delta_3 \neq 0,$	$\delta_4 = 0,$	$G(\eta) = -\frac{\delta_2}{\delta_3}.\,\mathrm{sech}^2\left(\frac{\sqrt{\delta_2}}{2}\eta\right).$

3. Methodology

Consider the Novikov-Veselov (NV) system

$$\begin{aligned} &\Psi_t + \alpha\Gamma_{xxy} + \beta\Phi_{xyy} + \gamma\Gamma_y\Phi + \gamma\left(\frac{\Psi^2}{2}\right)_y + \lambda\,\Gamma\,\Phi_x + \lambda\left(\frac{\Psi^2}{2}\right)_x = 0,\\ &\Gamma_y = \Psi_x,\\ &\Psi_y = \Phi_x, \end{aligned} \tag{3.1}$$

a system of PDEs in the unknown functions $\Psi = \Psi(x, y, t)$, $\Phi = \Phi(x, y, t)$, $\Gamma = \Gamma(x, y, t)$ and their partial derivatives. I plug the transformations

$$\begin{aligned} \Phi(x, y, t) =& \phi(\eta), \qquad\qquad \eta = x + y - wt,\\ \Psi(x, y, t) =& \psi(\eta),\\ \Gamma(x, y, t) =& \Theta(\eta), \end{aligned} \tag{3.2}$$

into Eq (3.1) to reduce it to a system of ODEs given by

$$\begin{aligned}
&-w\,\psi_\eta + \alpha\Theta_{\eta\eta\eta} + \beta\phi_{\eta\eta\eta} + \gamma\Theta_\eta\phi + \gamma\left(\frac{\psi^2}{2}\right)_\eta + \lambda\,\Theta\,\phi_\eta + \lambda\left(\frac{\psi^2}{2}\right)_\eta = 0,\\
&\Theta_\eta = \psi_\eta,\\
&\psi_\eta = \phi_\eta.
\end{aligned} \tag{3.3}$$

Integrating $\Theta_\eta = \psi_\eta$ and $\phi_\eta = \psi_\eta$ yields

$$\Theta = \psi, \qquad \text{and} \qquad \phi = \psi. \tag{3.4}$$

Substituting (3.4) into the first equation of (3.3) and integrating once with respect to η yields

$$-w\,\psi + (\alpha+\beta)\,\psi_{\eta\eta} + (\gamma+\lambda)\,\psi^2 = 0. \tag{3.5}$$

Balancing $\psi_{\eta\eta}$ with ψ^2 in (3.5) calculates the value of $N = 2$.

3.1. Application of modified F-expansion method

According to the modified F-expansion method with $N = 2$, the solutions of (3.5) are

$$\psi(\eta) = \rho_0 + \rho_1 F(\eta) + \frac{q_1}{F(\eta)} + \rho_2 F(\eta)^2 + \frac{q_2}{F(\eta)^2}, \tag{3.6}$$

and $F(\eta)$ is a solution of the following differential equation:

$$F'(\eta) = \mu_0 + \mu_1 F(\eta) + \mu_2 F(\eta)^2, \tag{3.7}$$

where μ_0, μ_1, μ_2 are given in Table 1. To explore the analytic solutions to (3.5), I ought to follow the subsequent steps.

Step 1. Placing (3.6) along with (3.7) into Eq (3.5) and gathering the coefficients of $F(\eta)^j$, j=$-4,-3,-2,-1,0,1,2,3,4$, to zeros gives a system of equations for $\rho_0,\ \rho_k,\ q_k,\ k = 1,2$.

Step 2. Solve the resulting system using mathematical software: for example, Mathematica or Maple.

Step 3. Choosing the values of $\mu_0,\ \mu_1$ and μ_2 and the function $F(\eta)$ from Table 1 and substituting them along with $\rho_0,\ \rho_k,\ q_k,\ k = 1,2$, in (3.6) produces a set of trigonometric function and rational solutions to (3.5).

Applying the above steps, I determine the values of $\rho_0,\ \rho_1,\ \rho_2,\ q_1,\ q_2$ and w as follows:

(1). When $\mu_0 = 0$, $\mu_1 = 1$ and $\mu_2 = -1$, I have two cases.

Case 1.

$$\rho_0 = 0, \quad \rho_1 = \frac{6(\alpha+\beta)}{\gamma+\lambda}, \quad \rho_2 = -\frac{6(\alpha+\beta)}{\gamma+\lambda}, \quad q_1 = q_2 = 0, \quad \text{and} \quad w = \alpha+\beta. \tag{3.8}$$

The solution is given by

$$\Psi_1(x,y,t) = \frac{3(\alpha+\beta)}{2(\gamma+\lambda)}\,\mathrm{sech}^2\left(\frac{1}{2}\,(x + y - (\alpha+\beta)t + x0)\right). \tag{3.9}$$

Case 2.

$$\rho_0 = -\frac{\alpha+\beta}{\gamma+\lambda}, \quad \rho_1 = \frac{6(\alpha+\beta)}{\gamma+\lambda}, \quad \rho_2 = -\frac{6(\alpha+\beta)}{\gamma+\lambda}, \quad q_1 = q_2 = 0, \quad \text{and} \quad w = -(\alpha+\beta). \tag{3.10}$$

The solution is given by

$$\Psi_2(x,y,t) = -\frac{(\alpha+\beta)}{2(\gamma+\lambda)}\left(3\tanh^2\left(\frac{1}{2}(x+y+t(\alpha+\beta)) + x0\right) - 1\right). \tag{3.11}$$

Figure 1 presents the time evolution of the analytic solutions (a) Ψ_1 and (b) Ψ_2 with $t = 0, 10, 20$. The parameter values are $x0 = -20$, $\alpha = 0.50, \beta = 0.6$, $\gamma = -1.5$, and $\lambda = 1$. Figure 2 presents the wave behavior by changing a certain parameter value and fixing the values of the others. Figure $2(a, b)$ presents the behavior of Ψ_1 when I change the values of (a) α or β and (b) γ or λ. In Figure $2(a)$ it can also be seen that the value of α or β affects the direction and amplitude of the wave, such that a negative value always makes the wave negative, its amplitude decreases when α, $\beta \to 0$, and its amplitude increases when α, $\beta \to \infty$. In Figure $2(b)$ the value of γ or λ affects the direction and amplitude of the wave, such that a negative value always makes the wave negative, and its amplitude decreases when the value of γ or λ increases. In Figure 2, (c) and (d) present the wave behavior of Ψ_2.

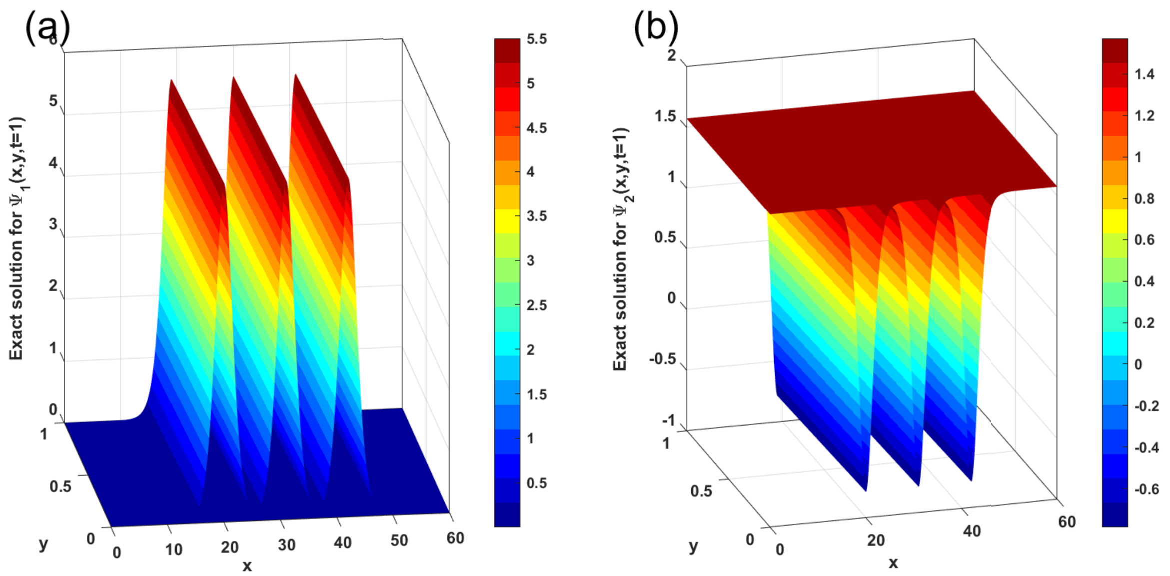

Figure 1. Time evolution of the analytic solutions (a) Ψ_1 and (b) Ψ_2 with $t = 0, 10, 20$. The parameter are given by $x0 = -20$, $\alpha = 0.50, \beta = 0.6$, $\gamma = -1.5$, and $\lambda = 1$.

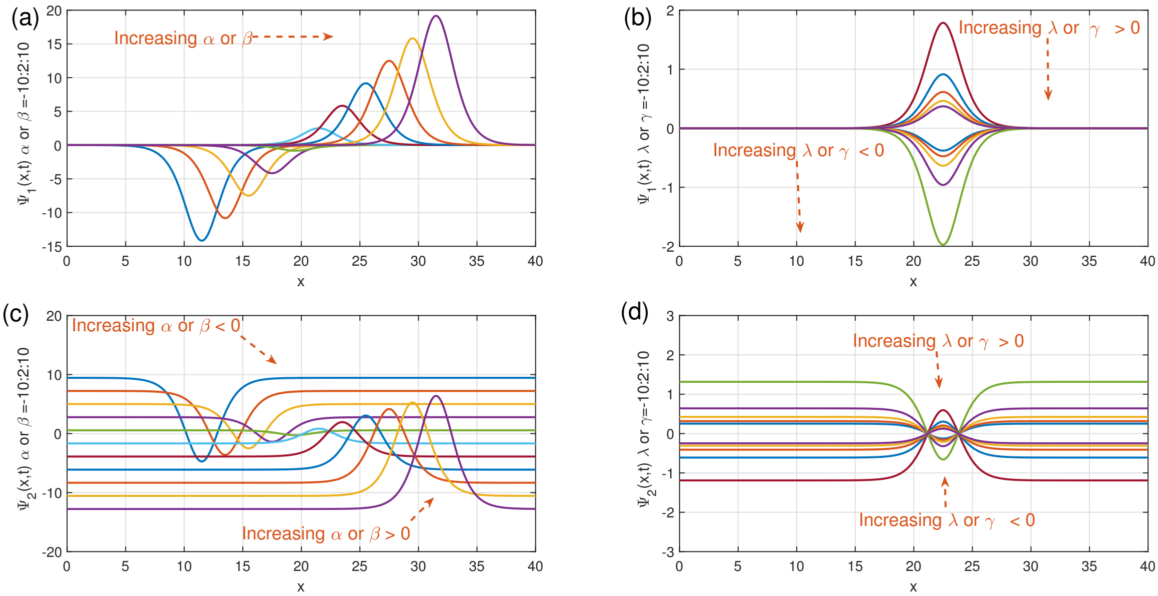

Figure 2. This figure present the wave behavior when changing a certain parameter value and fixing the values of the others. (a) presents the behavior when I change the value of α or β, and (b) presents when I change the value of γ or λ for the solution Ψ_1. (c) and (d) are for Ψ_2.

(2). When $\mu_0 = 0$, $\mu_1 = -1$, and $\mu_2 = 1$, I have two cases.

Case 3. The solution is given by

$$\Psi_3(x, y, t) = -\frac{3(\alpha+\beta)}{2(\gamma+\lambda)} \operatorname{csch}^2\left(\frac{1}{2}(x + y - (\alpha+\beta)t)\right). \tag{3.12}$$

Case 4. The solution is given by

$$\Psi_4(x, y, t) = -\frac{(\alpha+\beta)}{2(\gamma+\lambda)}\left(3\coth^2\left(\frac{1}{2}(x + y + t(\alpha+\beta))\right) - 1\right). \tag{3.13}$$

(3). When $\mu_0 = 1$, $\mu_1 = 0$, and $\mu_2 = -1$, I have

Case 5. The solution is given by

$$\Psi_5(x, y, t) = -\frac{8(\alpha+\beta)}{\gamma+\lambda}(\cosh(4(16t(\alpha+\beta) + x + y)) + 2)\operatorname{csch}^2(2(16t(\alpha+\beta) + x + y)). \tag{3.14}$$

(4). When $\mu_0 = \pm 1$, $\mu_1 = 0$, and $\mu_2 = \pm 1$, I have one case.

Case 6. The solution is given by

$$\Psi_6(x, y, t) = -\frac{24(\alpha+\beta)}{\gamma+\lambda}\csc^2(2(16t(\alpha+\beta) + x + y)). \tag{3.15}$$

3.2. Application of the generalized algebraic method

According to the generalized algebraic method, the solutions of (3.5) are given by the form

$$\psi(\eta) = \nu_0 + \nu_1 G(\eta) + \nu_2 G(\eta)^2 + \frac{r_1}{G(\eta)} + \frac{r_2}{G(\eta)^2}, \tag{3.16}$$

where ν_k, r_k are to be determined later. $G(\eta)$ is a solution of the following differential equation:

$$G'(\eta) = \varepsilon \sqrt{\sum_{k=0}^{4} \delta_k G^k(\eta)}, \tag{3.17}$$

where δ_k, $k = 0, 1, 3, 4$, are given in Table 2. In all the cases mentioned above and the subsequent solutions, I used the mathematical software Mathematica to find the values of the constants ν_0, ν_1, ν_2, r_1, r_2 and w. Thus, the analytic solutions to (3.5) using the generalized algebraic method will be presented here with different values of the constants δ_k, $k = 0, 1, 3, 4$.

(5). When $\delta_0 = \dfrac{\delta_2^2}{4\delta_4}$, $\delta_1 = \delta_3 = 0$, $\delta_2 < 0$, $\delta_4 > 0$, and $\varepsilon = \pm 1$,

$$\begin{aligned}
\nu_0 =& \frac{\pm\sqrt{4\delta_2^2\varepsilon^4(\alpha+\beta)^2(\gamma+\lambda)^2 - 3\delta_2\varepsilon^4(\alpha+\beta)^2(\gamma+\lambda)^2} - 2\delta_2\varepsilon^2(\alpha+\beta)(\gamma+\lambda)}{(\gamma+\lambda)^2},\\
\nu_2 =& -\frac{6\delta_4\varepsilon^2(\alpha+\beta)}{(\gamma+\lambda)},\\
\nu_1 =& r_1 = r_2 = 0, \quad \varepsilon = \pm 1.\\
w =& \pm\frac{2\sqrt{\left(4\delta_2^2 - 3\delta_2\right)\varepsilon^4(\alpha+\beta)^2(\gamma+\lambda)^2}}{(\gamma+\lambda)}.
\end{aligned} \tag{3.18}$$

Case 7. The solution is given by

$$\begin{aligned}
\Psi_7(x,y,t) = -\frac{1}{(\gamma+\lambda)^2}\Bigg(&-3\delta_2\varepsilon^4(\alpha+\beta)(\gamma+\lambda)\tanh^2\left(\frac{\sqrt{-\delta_2}\left(\frac{2t\sqrt{\delta_2(4\delta_2-3)\varepsilon^4(\alpha+\beta)^2(\gamma+\lambda)^2}}{\gamma+\lambda} + x + y\right)}{\sqrt{2}}\right)\\
&+2\delta_2\varepsilon^2(\alpha+\beta)(\gamma+\lambda) + \sqrt{\delta_2(4\delta_2-3)\varepsilon^4(\alpha+\beta)^2(\gamma+\lambda)^2}\Bigg).
\end{aligned} \tag{3.19}$$

Figure 3 shows the time evolution of the analytic solutions. Figure 3(a) shows Ψ_7 with t=0 : 2 : 6. The parameter values are $\delta_2 = -1$, $\delta_4 = 1$, $\epsilon = -1$, $\alpha = 0.50$, $\beta = 0.6$, $\gamma = -1.5$, $\lambda = 1.8$ and $x0 = -10$. Figure 3(b) shows Ψ_8 with $t = 0 : 2 : 8$. The parameter values are $\delta_2 = 1$, $\delta_4 = -1$, $\epsilon = -1$, $\alpha = 0.50$, $\beta = 0.6$, $\gamma = -1.5$, $\lambda = 1.8$ and $x0 = -10$. Figures 4–6 present the $3D$ time evolution of the analytic solutions Ψ_2 (left) and the numerical solutions (right) obtained employing the scheme 5.1 with $t = 5, 15, 25$, $M_x = 1600$, $N_y = 100$, $x = 0 \to 60$ and $y = 0 \to 1$.

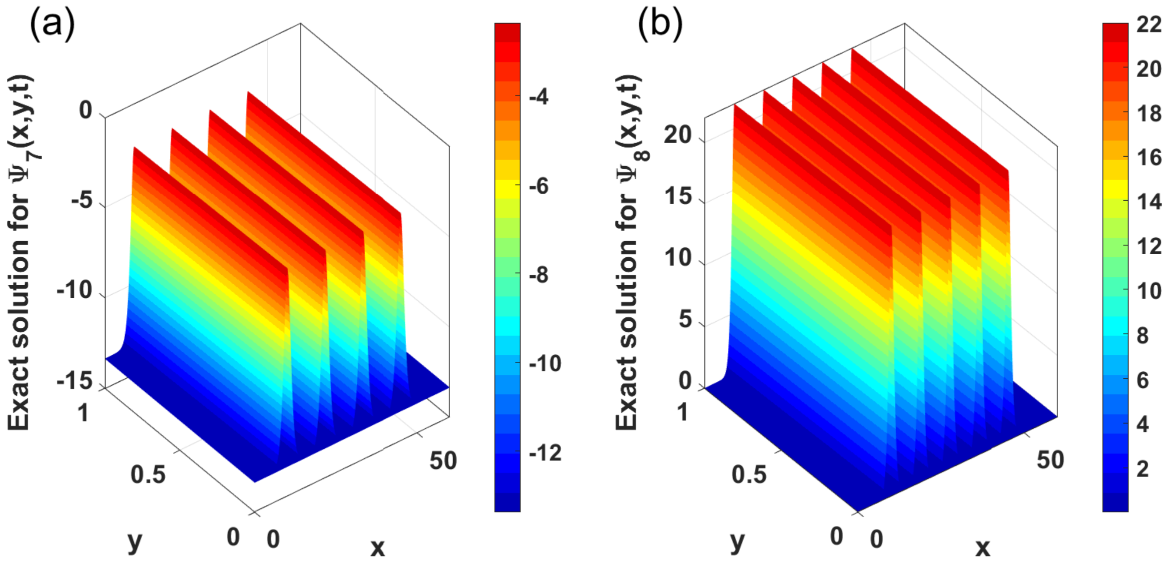

Figure 3. Time evolution of the analytic solutions. (a) Ψ_7 with $t = 0:2:6$. The parameter values are $\delta_2 = -1$, $\delta_4 = 1$, $\epsilon = -1$, $\alpha = 0.50$, $\beta = 0.6$, $\gamma = -1.5$, $\lambda = 1.8$ and $x0 = -10$. (b) Ψ_8 with $t = 0:2:8$. The parameter values are $\delta_2 = 1$, $\delta_4 = -1$, $\epsilon = -1$, $\alpha = 0.50$, $\beta = 0.6$, $\gamma = -1.5$, $\lambda = 1.8$ and $x0 = -10$.

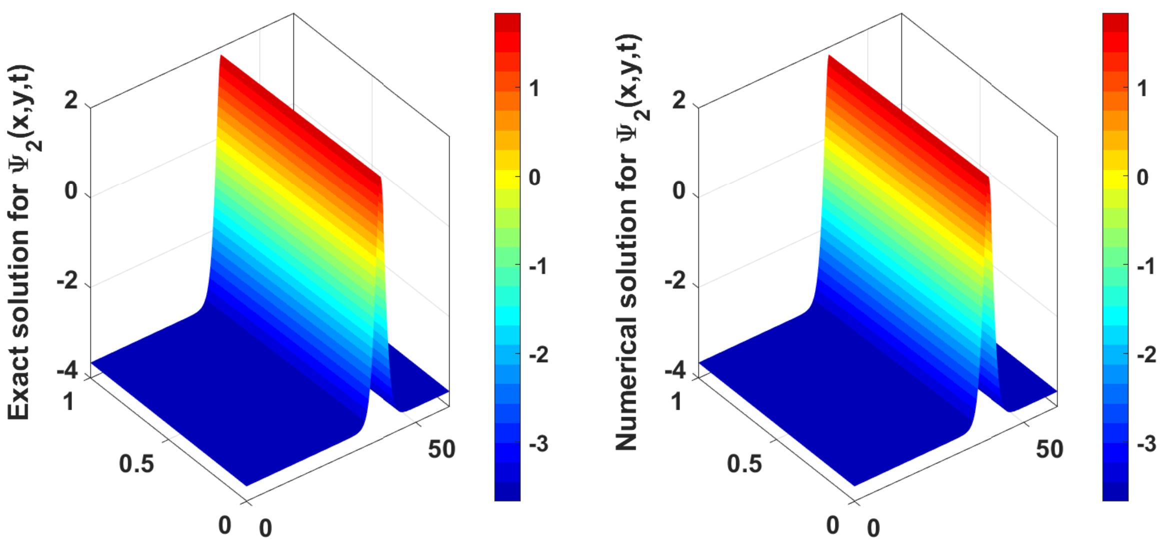

Figure 4. 3D graphs presenting the analytic (left) and the numerical (right) solutions of $\Psi_2(x, y, t)$ at $t = 5$. The figures present the strength of agreement between analytic and numerical solutions.

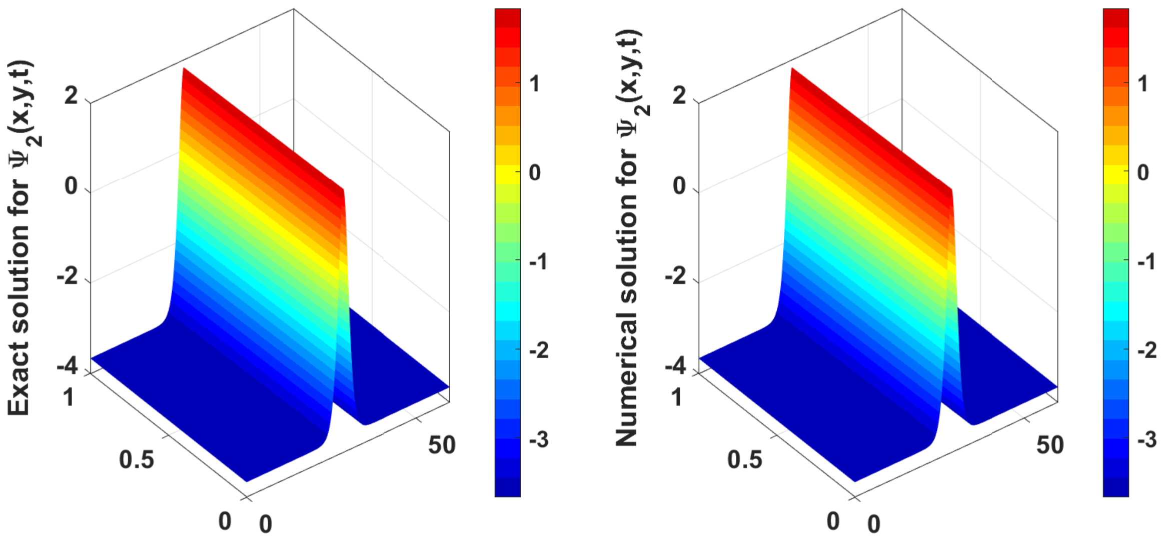

Figure 5. 3D graphs presenting the analytic (left) and the numerical (right) solutions of $\Psi_2(x, y, t)$ at $t = 15$. The figures present the strength of agreement between analytic and numerical solutions.

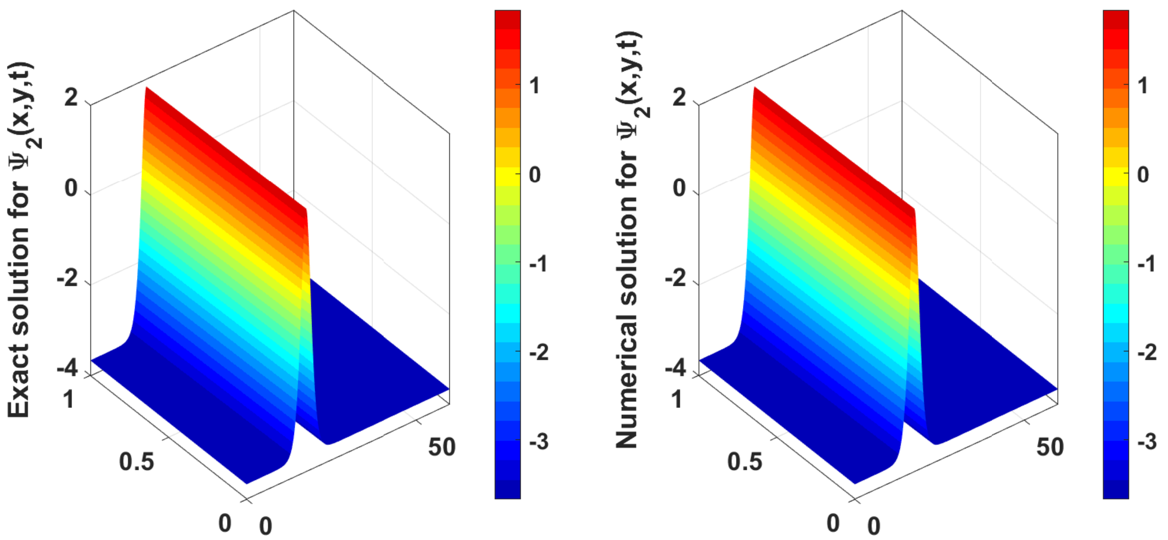

Figure 6. 3D graphs presenting the analytic (left) and the numerical (right) solutions of $\Psi_2(x, y, t)$ at $t = 25$. The figures present the strength of agreement between analytic and numerical solutions.

(6). When $\delta_0 = 0$, $\delta_1 = \delta_3 = 0$, $\delta_2 > 0$, $\delta_4 < 0$, and $\varepsilon = \pm 1$,

$$v_2 = -\frac{6\delta_4\varepsilon^2(\alpha+\beta)}{\gamma+\lambda}, \quad v_1 = v_0 = r_1 = r_2 = 0, \quad w = 4\delta_2\varepsilon^2(\alpha+\beta). \tag{3.20}$$

Case 8. The solution is given by

$$\Psi_8(x,y,t) = \frac{6\delta_2\epsilon^4(\alpha+\beta)\,\mathrm{sech}^2\left(\sqrt{\delta_2}\left(-4\delta_2\epsilon^2 t(\alpha+\beta)+x+y\right)\right)}{\gamma+\lambda} \tag{3.21}$$

(7). When $\delta_0 = 0, \delta_1 = \delta_4 = 0, \delta_3 \neq 0, \delta_2 > 0, \varepsilon = \pm 1$

$$\begin{aligned} &\text{Set 1. } \nu_1 = -\tfrac{3\delta_3\varepsilon^2(\alpha+\beta)}{2(\gamma+\lambda)},\ \nu_0 = \nu_2 = r_1 = r_2 = 0,\ w = \delta_2\varepsilon^2(\alpha+\beta). \\ &\text{Set 2. } \nu_0 = -\tfrac{\delta_2\varepsilon^2(\alpha+\beta)}{(\gamma+\lambda)},\ \nu_1 = -\tfrac{3\delta_3\varepsilon^2(\alpha+\beta)}{2(\gamma+\lambda)},\quad \nu_2 = r_1 = r_2 = 0,\ w = -\delta_2\varepsilon^2(\alpha+\beta). \end{aligned} \tag{3.22}$$

Case 9. The solution is given by

$$\Psi_9(x,y,t) = \frac{3\delta_2(\alpha+\beta)\,\mathrm{sech}^2\left(\frac{1}{2}\sqrt{\delta_2}(\delta_2 t(-(\alpha+\beta))+x+y)\right)}{2(\gamma+\lambda)}. \tag{3.23}$$

Case 10. The solution is given by

$$\Psi_{10}(x,y,t) = \frac{3\delta_2(\alpha+\beta)\,\mathrm{sech}^2\left(\frac{1}{2}\sqrt{\delta_2}(\delta_2 t(\alpha+\beta)+x+y)\right)}{2(\gamma+\lambda)} - \frac{\delta_2(\alpha+\beta)}{\gamma+\lambda}. \tag{3.24}$$

4. Numerical solution

In this section I extract numerical solutions to the resulting ODE system (3.5) using several numerical methods. The purpose of this procedure is to guarantee the accuracy of the analytic solutions. I picked one of the analytic solutions above to be a sample, (3.11). The nonlinear shooting and BVP methods, at $t = 0$, are used by taking the value of ψ at the right endpoint of the domain $\eta = 0$ with guessing the initial value for ψ_η. The new target is to obtain the second boundary condition of ψ at the left endpoint of a particular domain. Once the numerical result is obtained, I compare it with the analytic solution (3.11). The MATLAB solver ODE15s and FSOLVE [47] are used to get the numerical solution. The resulting ODE (3.5) is discretized as

$$f(\psi) = 0, \qquad f(\psi_i) = -w\,\psi_i + \frac{\alpha+\beta}{\Delta_\eta}(\psi_{i+1} - 2\psi_i + \psi_{i-1}) + \frac{\gamma+\lambda}{2\Delta_\eta}\left(\psi_{i+1}^2 - \psi_{i-1}^2\right), \tag{4.1}$$

for the BVP method and

$$\psi_{\eta\eta} = \frac{1}{\alpha+\beta}\left(w\psi - (\gamma+\lambda)\psi^2\right), \tag{4.2}$$

for the shooting method. Figure 7 presents the comparison between the numerical solutions obtained using the above numerical methods and the analytic solution. Figure 7 shows that the solutions are identical to the analytic solution.

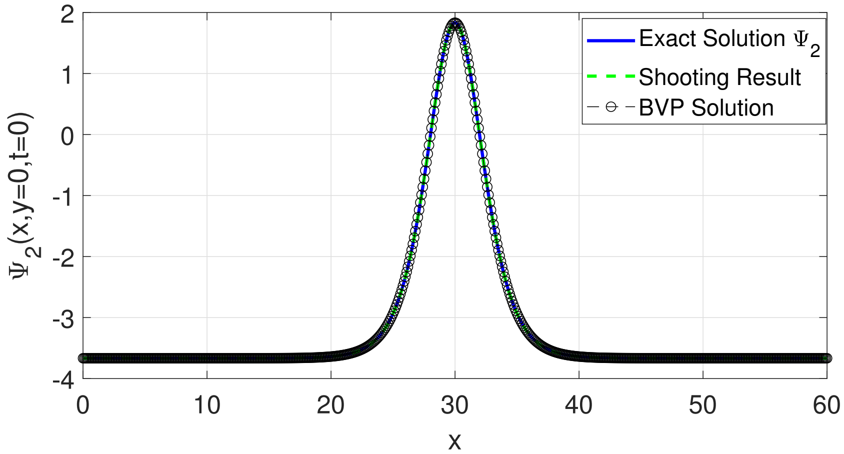

Figure 7. Comparing the numerical solutions resulting from the shooting and BVP methods with the analytic solution (3.11) at $t = 0$. The parameter values are taken as $\alpha = 0.50, \beta = 0.6$, $\gamma = -1.5, \lambda = 1.8$, with $N = 600$.

Thus, it is possible to verify the correctness of the analytic solution. I also accept the obtained numerical solution as an initial condition for the numerical scheme in the next section.

5. Numerical scheme on a fixed mesh

In this section, I use the finite-difference method to obtain the numerical results of system (1.1) over the domain $[a, b] \times [c, d]$. Here, $a,\ b,\ c$ and d represent the endpoints of the rectangular domain in the x and y directions, respectively, and T_f is a certain time. The domain $[a, b] \times [c, d]$ is split into $(M_x + 1) \times (N_y + 1)$ mesh points:

$$\begin{aligned} x_m &= a + m\,\Delta_x, \qquad m = 0,\ 1,\ 2,\ \ldots,\ M_x, \\ y_n &= c + n\,\Delta_y, \qquad n = 0,\ 1,\ 2,\ \ldots,\ N_y, \end{aligned}$$

where Δ_x and Δ_y are the step-sizes of the x and y domains, respectively. The system (1.1) is converted to an ODE system by discretizing the space derivatives while keeping the time derivative continuous. Completing this yields

$$\begin{aligned} &\Psi_t|^k_{m,n} + \frac{\alpha}{2\Delta_y\Delta_x^2}\delta_x^2\left(\Gamma^{k+1}_{m,n+1} - \Gamma^{k+1}_{m,n-1}\right) + \frac{\beta}{2\Delta_x\Delta_y^2}\delta_y^2\left(\Phi^{k+1}_{m+1,n} - \Phi^{k+1}_{m-1,n}\right) \\ &\quad - \frac{\gamma}{4\Delta_y}\left(\left(\Phi^{k+1}_{m,n+1} + \Phi^{k+1}_{m,n}\right)\Gamma^{k+1}_{m,n+1} - \left(\Phi^{k+1}_{m,n} + \Phi^{k+1}_{m,n-1}\right)\Gamma^{k+1}_{m,n-1}\right) \\ &\quad - \frac{\lambda}{4\Delta_x}\left(\left(\Gamma^{k+1}_{m+1,n} + \Gamma^{k+1}_{m,n}\right)\Phi^{k+1}_{m+1,n} - \left(\Gamma^{k+1}_{m,n} + \Gamma^{k+1}_{m-1,n}\right)\Phi^{k+1}_{m-1,n}\right) \\ &\quad + \frac{\gamma}{4\Delta_y}\left(\left(\Psi^{k+1}_{m,n+1}\right)^2 - \left(\Psi^{k+1}_{m,n-1}\right)^2\right) + \frac{\lambda}{4\Delta_x}\left(\left(\Psi^{k+1}_{m+1,n}\right)^2 - \left(\Psi^{k+1}_{m-1,n}\right)^2\right) = 0, \\ &\frac{1}{2\Delta_y}(\Gamma^{k+1}_{m,n+1} - \Gamma^{k+1}_{m,n-1}) = \frac{1}{2\Delta_x}(\Psi^{k+1}_{m+1,n} - \Psi^{k+1}_{m-1,n}), \\ &\frac{1}{2\Delta_y}(\Psi^{k+1}_{m,n+1} - \Psi^{k+1}_{m,n-1}) = \frac{1}{2\Delta_x}(\Phi^{k+1}_{m+1,n} - \Phi^{k+1}_{m-1,n}), \end{aligned} \tag{5.1}$$

where

$$\delta_x^2 \Gamma_{m,n}^{k+1} = \left(\Gamma_{m+1,n}^{k+1} - 2\Gamma_{m,n}^{k+1} + \Gamma_{m-1,n}^{k+1} \right),$$
$$\delta_y^2 \Phi_{m,n}^{k+1} = \left(\Phi_{m,n+1}^{k+1} - 2\Phi_{m,n}^{k+1} + \Phi_{m,n-1}^{k+1} \right),$$

subject to the boundary conditions:

$$\begin{aligned} \Psi_x(a,\, y,\, t) &= \Psi_x(b,\, y,\, t) = 0, \qquad \forall y \in [c,\, d], \\ \Psi_y(x,\, c,\, t) &= \Psi_y(x,\, d,\, t) = 0, \quad \forall x \in [a,\, b]. \end{aligned} \tag{5.2}$$

Equation (5.2) permits us to use fictitious points in estimating the space derivatives at the domain's endpoints. The initial conditions are generated by

$$\Psi_2(x, y, 0) = -\frac{(\alpha+\beta)}{2(\gamma+\lambda)} \left(3\tanh^2\left(\frac{1}{2}(x+y+x0 \right) - 1 \right), \tag{5.3}$$

where α, β, γ and λ are user-defined parameters. In all the numerical results shown in this section, the parameter values are fixed as $\alpha = 0.50$, $\beta = 0.6$, $\gamma = -1.50$, $\lambda = 1.80$, $x0 = -45.0$, $y = 0 \rightarrow 1$, $x = 0 \rightarrow 60$ and $t = 0 \rightarrow 25$. The above system is solved by using an ODE solver in FORTRAN called the DDASPK solver [48]. This solver used a backward differentiation formula. Since I do not have the initial conditions for the space derivatives, I approximate the Jacobian matrix of the linearized system by using LU-Factorization. The obtained numerical results are acceptable. This can be observed from the Figures 8 and 9.

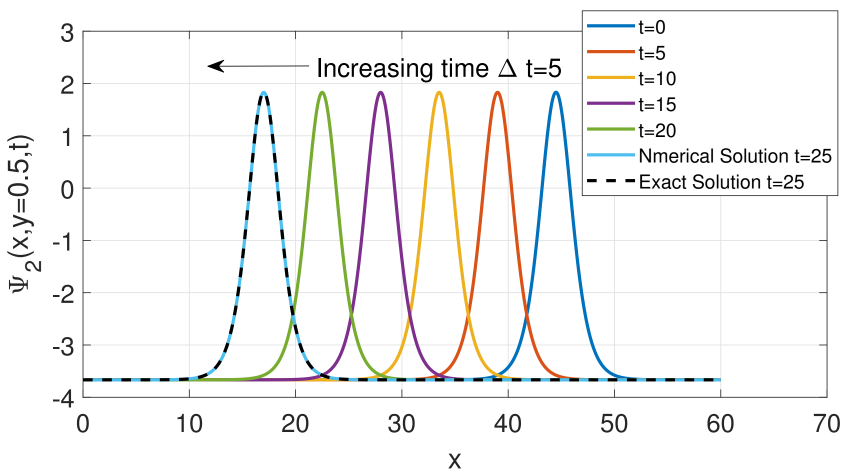

Figure 8. Time change for the numerical results while holding $y = 0.5$ and $M_x = 1600$ at $t = 0 : 5 : 25$. The wave at $t = 25$ illustrates that the numerical and the analytic solutions are quite identical.

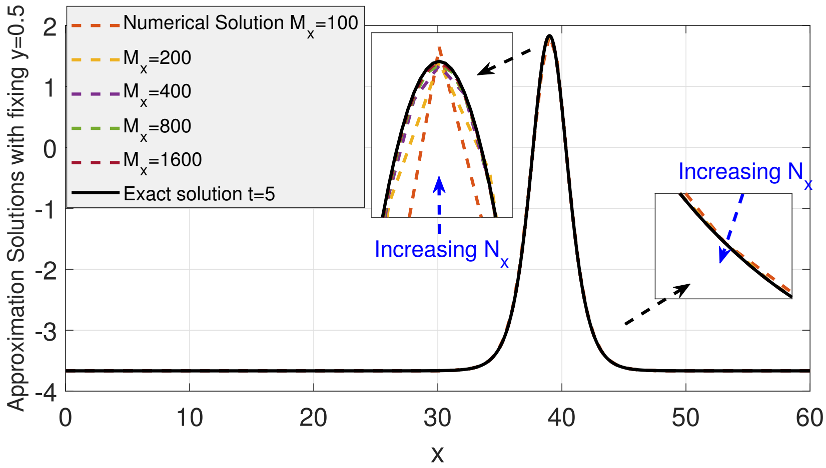

Figure 9. The convergence histories of the scheme with the fixation of both $y = 0.5$ and $M_x = 1600$ at $t = 5$.

6. Stability of the numerical scheme

The von Neumann analysis is used to examine the stability of the scheme (5.1). The von Neumann analysis is occasionally called Fourier analysis and is utilized exclusively when the scheme is linear. Hence, I suppose that the linear version is given by

$$\begin{aligned} &\Psi_t + \alpha\Gamma_{xxy} + \beta\Phi_{xyy} + s_0\,\Gamma_y + s_1\,\Psi_y + s_2\,\Phi_x + s_3\,\Psi_x = 0,\\ &\Gamma_y = \Psi_x,\\ &\Psi_y = \Phi_x, \end{aligned} \tag{6.1}$$

where $s_0 = \gamma\Phi$, $s_1 = \gamma\Psi$, $s_2 = \lambda\Gamma$, $s_3 = \lambda\Psi$ are constants. Since $\Gamma_y = \Psi_x$, and $\Psi_y = \Phi_x$, the first equation of (6.1) is given by

$$\Psi_t + \alpha\Psi_{xxx} + \beta\Psi_{yyy} + s_0\,\Psi_y + s_1\,\Psi_y + s_2\,\Psi_x + s_3\,\Psi_x = 0, \tag{6.2}$$

where α, β, γ, λ, s_0, s_1, s_2, s_3, l_4 are constants. I set directly

$$\Psi^k_{m,n} = \mu^k\,\exp(\iota\,\pi\,\xi_0\,n\,\Delta_x)\exp(\iota\,\pi\,\xi_1\,m\,\Delta_y), \tag{6.3}$$

and also I can have

$$\begin{aligned} \Psi^{k+1}_{m,n} =& \mu\,\Psi^k_{m,n}, \quad \Psi^k_{m+1,n} = \exp(\iota\,\pi\,\xi_0\,\Delta_x)\,\Psi^k_{m,n}, \quad \Psi^k_{m,n+1} = \exp(\iota\,\pi\,\xi_1\,\Delta_y)\,\Psi^k_{m,n},\\ &\Psi^k_{m-1,n} = \exp(-\iota\,\pi\,\xi_0\,\Delta_x)\,\Psi^k_{m,n}, \quad \Psi^k_{m,n-1} = \exp(-\iota\,\pi\,\xi_1\,\Delta_y)\,\Psi^k_{m,n},\\ m =& 1,\,2,\ldots,\,N_x - 1, \qquad n = 1,2,\ldots,\,N_y - 1. \end{aligned}$$

Substituting (6.3) into (6.2) and doing some operations, I have

$$1 = \mu\left(1 - \iota\Delta_t\left(\frac{\sin(\xi_0\pi\Delta_x)}{\Delta_x}\left(\frac{4\,\alpha}{\Delta_x^2}\,\sin^2(\tfrac{\xi_0\pi\,\Delta_x}{2}) - s_2 - s_3\right) + \frac{\sin(\xi_1\pi\Delta_y)}{\Delta_y}\left(\frac{4\,\beta}{\Delta_y^2}\,\sin^2(\tfrac{\xi_1\pi\,\Delta_y}{2}) - s_0 - s_1\right)\right)\right).$$

Hence,

$$\mu = \frac{1}{1 - a\iota}, \tag{6.4}$$

where

$$a = \Delta_t \left(\frac{\sin(\xi_0 \pi \Delta_x)}{\Delta_x} \left(\frac{4\,\alpha}{\Delta_x^2} \sin^2(\tfrac{\xi_0 \pi\, \Delta_x}{2}) - s_2 - s_3 \right) + \frac{\sin(\xi_1 \pi \Delta_y)}{\Delta_y} \left(\frac{4\beta}{\Delta_y^2} \sin^2(\tfrac{\xi_1 \pi\, \Delta_y}{2}) - s_0 - s_1 \right) \right).$$

Thus,

$$|\mu|^2 = \frac{1}{1 + a^2} \leq 1. \tag{6.5}$$

The stability condition of the von Neumann analysis is fulfilled. Consequently, from Eq (6.5), the scheme is unconditionally stable.

7. Error analysis

To examine the accuracy of the numerical scheme (5.1), I study the truncation error utilizing Taylor expansions. Suppose that the error is

$$e_{m,n}^{k+1} = \Psi_{m,n}^{k+1} - \Psi(x_m, y_n, t_{k+1}), \tag{7.1}$$

where $\Psi(x_m, y_n, t_{k+1})$ and $\Psi_{m,n}^{k+1}$ are the analytic solution and an approximate solution, respectively. Substituting (7.1) into (5.1) gives

$$\begin{aligned} \frac{e_{j,k}^{k+1} - e_{j,k}^{k}}{\Delta_t} =& T_{m,n}^{k+1} - \left(\alpha \frac{1}{2\Delta_x^3} \delta_x^2 \left(e_{m+1,n}^{k+1} - e_{m-1,n}^{k+1} \right) + \beta \frac{1}{2\Delta_y^3} \delta_y^2 \left(e_{m,n+1}^{k+1} - e_{m,n-1}^{k+1} \right) \right. \\ & \left. + \frac{s_2 + s_3}{2\Delta_x} \left(e_{m+1,n}^{k+1} - e_{m-1,n}^{k+1} \right) + \frac{s_0 + s_1}{2\Delta_y} \left(e_{m,n+1}^{k+1} - e_{m,n-1}^{k+1} \right) \right), \end{aligned}$$

where

$$\begin{aligned} T_{m,n}^{k+1} =& \frac{\alpha}{2\Delta_x^3} \delta_x^2 \left(\Psi(x_{m+1}, y_n, t_{k+1}) - \Psi(x_{m-1}, y_n, t_{k+1}) \right) + \frac{\beta}{2\Delta_y^3} \delta_y^2 \left(\Psi(x_m, y_{n+1}, t_{k+1}) - \Psi(x_m, y_{n-1}, t_{k+1}) \right) \\ & + \frac{s_2 + s_3}{2\Delta_x} \left(\Psi(x_{m+1}, y_n, t_{k+1}) - \Psi(x_{m-1}, y_n, t_{k+1}) \right) + \frac{s_0 + s_1}{2\Delta_y} \left(\Psi(x_m, y_{n+1}, t_{k+1}) - \Psi(x_m, y_{n-1}, t_{k+1}) \right). \end{aligned}$$

Hence,

$$\begin{aligned} T_{m,n}^{k+1} \leq& \frac{\Delta_t}{2} \frac{\partial^2 \Psi(x_m, y_n, \xi_{k+1})}{\partial t^2} - \frac{\Delta_x^2}{2} \frac{\partial^5 \Psi(\zeta_m, y_n, t_{k+1})}{\partial x^5} - \frac{\Delta_y^2}{2} \frac{\partial^5 \Psi(x_m, \eta_n, t_{k+1})}{\partial x^5} \\ & - \frac{\Delta_y^2}{6} \frac{\partial^3 \Psi(x_m, \eta_n, t_{k+1})}{\partial x^3} - \frac{\Delta_x^2}{6} \frac{\partial^3 \Psi(\zeta_m, y_n, t_{k+1})}{\partial x^3}. \end{aligned}$$

Accordingly, the truncation error of the numerical scheme is

$$T_{m,n}^{k+1} = O(\Delta_t, \Delta_x^2, \Delta_y^2).$$

8. Results and discussion

I have prosperously employed several analytical methods to extract the traveling wave solutions to the two-dimensional Novikov-Veselov system, confirming the solutions with numerical results obtained using the numerical scheme (5.1). The major highlights of the results are shown in Table 3 and Figures 8–10, which allow immediate comparison of the analytic solutions with the numerical results. Through these, I can notice that the solutions are identical to a large extent, and the error approaches zero whenever the value of $\Delta_x, \Delta_y \to 0$. The numerical schemes are unconditionally stable for fixing the parameter values $\alpha = 0.50$, $\beta = 0.6$, $\gamma = -1.50$, $\lambda = 1.80$, $x0 = -45.0$, $y = 0 \to 1$, $x = 0 \to 60$ and $t = 0 \to 25$.

Table 3. The relative error with L_2 norm and CPU at $t = 20$.

Δ_x	The Relative Error	CPU
0.6000	5.600×10^{-3}	0.063×10^3 m
0.3000	2.100×10^{-3}	0.1524×10^3 s
0.1500	6.700×10^{-4}	0.3564×10^3 s
0.0750	2.100×10^{-4}	0.8892×10^3 s
0.0375	6.610×10^{-5}	1.7424×10^3 s
0.0187	2.310×10^{-5}	4.0230×10^3 s

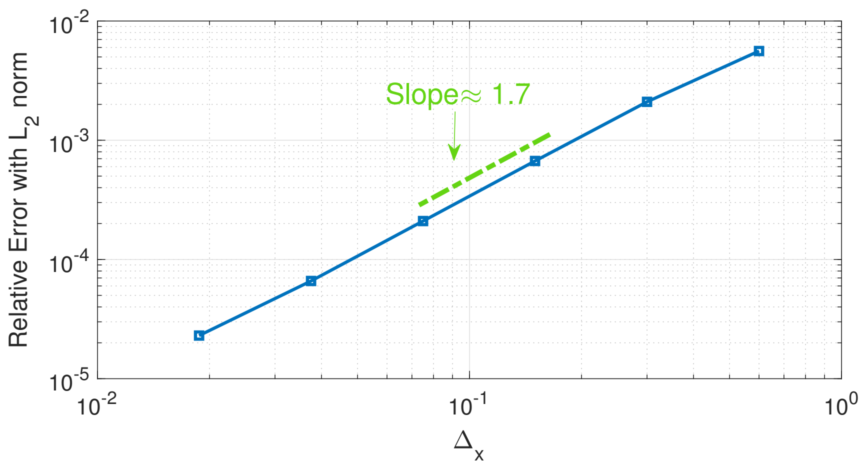

Figure 10. The convergence histories measured utilizing the relative error with l_2 norm as a function of Δ_x (see Table 3). Here, I picked a certain value of the variable $y = 0.5$ at $t = 20$ and $x = 0 \to 60$.

Figure 1 presents the time evolution of the analytic solutions (a) Ψ_1 and (b) Ψ_2 with $t = 0, 10, 20$. The parameter values are $x0 = -20$, $\alpha = 0.50$, $\beta = 0.6$, $\gamma = -1.5$, and $\lambda = 1$. Figure 2 presents the wave behavior by changing a certain parameter value and fixing the values of the others. Figure $2(a, b)$ presents the behavior of Ψ_1 when I change the values of (a) α or β and (b) γ or λ. In Figure $2(a)$ it can also be seen that the value of α or β affects the direction and amplitude of the wave, such that a negative value always makes the wave negative, its amplitude decreases when $\alpha, \beta \to 0$, and its amplitude increases when $\alpha, \beta \to \infty$. In Figure $2(b)$ the value of γ or λ affects the direction and amplitude of the wave, such that a negative value always makes the wave negative, and its amplitude decreases when the value of γ or λ increases. In Figure 2(c, d) present the wave behavior of Ψ_2. Figure 3 shows the time evolution of the analytic solutions. Figure 3(a) shows Ψ_7 with $t = 0 : 2 : 6$. The parameter values are $\delta_2 = -1$, $\delta_4 = 1$, $\epsilon = -1$, $\alpha = 0.50$, $\beta = 0.6$, $\gamma = -1.5$, $\lambda = 1.8$ and $x0 = -10$. Figure 3(b) shows Ψ_8 with $t = 0 : 2 : 8$. The parameter values are $\delta_2 = 1$, $\delta_4 = -1$, $\epsilon = -1$, $\alpha = 0.50$, $\beta = 0.6$, $\gamma = -1.5$, $\lambda = 1.8$ and $x0 = -10$. Figures 4–6 present the $3D$ time evolution of the analytic solutions Ψ_2 (left) and the numerical solutions (right) obtained employing the scheme 5.1 with $t = 5, 15, 25$, $M_x = 1600$, $N_y = 100$, $x = 0 \to 60$ and $y = 0 \to 1$. These figures provide us with an adequate answer that the numerical and analytic solutions are quite identical. Barman et al. [42] accepted several traveling wave solutions for (1.1) as hyperbolic functions. The authors employed other parameters to develop new forms for the accepted solution. They proposed that Eq (1.1) describes tidal and tsunami waves, electromagnetic waves in transmission cables and magneto-sound and ion waves in plasma. In comparison, I have found numerous solutions also as hyperbolic functions. Furthermore, I obtained the numerical solutions to enhance the assurance that the solutions presented here are correct and accurate.

9. Conclusions

I have successfully utilized the generalized algebraic and modified F-expansion methods to acquire the soliton solutions for the two-dimensional Novikov-Veselov system, verifying these solutions with numerical results obtained by employing the numerical scheme (5.1). The major highlights of the results shown in Figures 8–10 and Table 3, which allow immediate comparison of the analytic solutions with the numerical results. Through these, I can notice that the solutions are identical to a large extent, and the error approaches zero whenever the value of $\Delta_x, \Delta_y \to 0$. The numerical schemes are unconditionally stable for fixing the parameter values $\alpha = 0.50$, $\beta = 0.6$, $\gamma = -1.50$, $\lambda = 1.80$, $x0 = -45.0$, $y = 0 \to 1$, $x = 0 \to 60$ and $t = 0 \to 25$. The Jacobi elliptic functions have effectively deteriorated to hyperbolic functions. The applied numerical schemes have provided reliable numerical solutions when using a small value of $\Delta_x, \Delta_y \to 0$.

Ultimately, I can deduce that the methods used are valuable and applicable to extract soliton solutions for other nonlinear evolutionary systems found in chemistry, engineering, physics and other sciences.

Conflict of interest

The author declares that he has no potential conflict of interest in this article.

References

1. A. Aasaraai, The application of modified F-expansion method solving the Maccari's system, *Journal of Advances in Mathematics and Computer Science*, **11** (2015), 1–14. http://dx.doi.org/10.9734/BJMCS/2015/19938

2. C. Bai, C. Bai, H. Zhao, A new generalized algebraic method and its application in nonlinear evolution equations with variable coefficients, *Z. Naturforsch. A*, **60** (2005), 211–220. https://doi.org/10.1515/zna-2005-0401
3. A. Bekir, O. Unsal, Analytic treatment of nonlinear evolution equations using first integral method, *Pramana-J. Phys.*, **79** (2012), 3–17. http://dx.doi.org/10.1007/s12043-012-0282-9
4. D. Kumar, A. Seadawy, A. Joardar, Modified Kudryashov method via new exact solutions for some conformable fractional differential equations arising in mathematical biology, *Chinese J. Phys.*, **56** (2018), 75–85. http://dx.doi.org/10.1016/j.cjph.2017.11.020
5. G. Adomain, *Solving frontier problems of physics: the decomposition method*, Dordrecht: Springer, 1994. http://dx.doi.org/10.1007/978-94-015-8289-6
6. X. Feng, Exploratory approach to explicit solution of nonlinear evolutions equations, *Int. J. Theor. Phys.*, **39** (2000), 207–222. http://dx.doi.org/10.1023/A:1003615705115
7. A. Alharbi, M. Almatrafi, Numerical investigation of the dispersive long wave equation using an adaptive moving mesh method and its stability, *Results Phys.*, **16** (2020), 102870. http://dx.doi.org/10.1016/j.rinp.2019.102870
8. A. Alharbi, M. Almatrafi, Riccati-Bernoulli sub-ODE approach on the partial differential equations and applications, *Int. J. Math. Comput. Sci.*, **15** (2020), 367–388.
9. A. Alharbi, M. Almatrafi, New exact and numerical solutions with their stability for Ito integro-differential equation via Riccati–Bernoulli sub-ODE method, *J. Taibah Univ. Sci.*, **14** (2020), 1447–1456. http://dx.doi.org/10.1080/16583655.2020.1827853
10. A. Alharbi, M. Almatrafi, Exact and numerical solitary wave structures to the variant Boussinesq system, *Symmetry*, **12** (2020), 1473. http://dx.doi.org/10.3390/sym12091473
11. M. Almatrafi, A. Alharbi, C. Tunç, Constructions of the soliton solutions to the good Boussinesq equation, *Adv. Differ. Equ.*, **2020** (2020), 629. http://dx.doi.org/10.1186/s13662-020-03089-8
12. A. Alharbi, M. Almatrafi, A. Seadawy, Construction of the numerical and analytical wave solutions of the Joseph-Egri dynamical equation for the long waves in nonlinear dispersive systems, *Int. J. Mod. Phys. B*, **34** (2020), 2050289. http://dx.doi.org/10.1142/S0217979220502896
13. A. Alharbi, M. Almatrafi, Kh. Lotfy, Constructions of solitary travelling wave solutions for Ito integro-differential equation arising in plasma physics, *Results Phys.*, **19** (2020), 103533. http://dx.doi.org/10.1016/j.rinp.2020.103533
14. A. Alharbi, M. Almatrafi, Exact solitary wave and numerical solutions for geophysical KdV equation, *J. King Saud Univ. Sci.*, **34** (2022), 102087. http://dx.doi.org/10.1016/j.jksus.2022.102087
15. S. Tian, J. Tu, T. Zhang, Y. Chen, Integrable discretizations and soliton solutions of an Eckhaus-Kundu equation, *Appl. Math. Lett.*, **122** (2021), 107507. http://dx.doi.org/10.1016/j.aml.2021.107507
16. S. Tian, M. Xu, T. Zhang, A symmetry-preserving difference scheme and analytical solutions of a generalized higher-order beam equation, *Proc. R. Soc. A.*, **477** (2021), 20210455. http://dx.doi.org/10.1098/rspa.2021.0455

17. S. Tian, Lie symmetry analysis, conservation laws and solitary wave solutions to a fourth-order nonlinear generalized Boussinesq water wave equation, *Appl. Math. Lett.*, **100** (2020), 106056. http://dx.doi.org/10.1016/j.aml.2019.106056

18. S. Tian, D. Guo, X. Wang, T. Zhang, Traveling wave, lump wave, rogue wave, multi-kink solitary wave and interaction solutions in a (3+1)-dimensional Kadomtsev-Petviashvili equation with Bäcklund transformation, *J. Appl. Anal. Comput.*, **11** (2021), 45–58. http://dx.doi.org/10.11948/20190086

19. J. Yang, S. Tian, Z. Li, Riemann-Hilbert problem for the focusing nonlinear Schrödinger equation with multiple high-order poles under nonzero boundary conditions, *Physica D*, **432** (2022), 133162. http://dx.doi.org/10.1016/j.physd.2022.133162

20. X. Gao, Y. Guo, W. Shan, Optical waves/modes in a multicomponent inhomogeneous optical fiber via a three-coupled variable-coefficient nonlinear Schrödinger system, *Appl. Math. Lett.*, **120** (2021), 107161. http://dx.doi.org/10.1016/j.aml.2021.107161

21. X. Gao, Y. Guo, W. Shan, In nonlinear optics, fluid mechanics, plasma physics or atmospheric science: symbolic computation on a generalized variable-coefficient Korteweg-de Vries equation, *Acta Math. Sin.-English Ser.*, in press. http://dx.doi.org/10.1007/s10114-022-9778-5

22. X. Gao, Y. Guo, W. Shan, Similarity reductions for a generalized (3+1)-dimensional variable-coefficient B-type Kadomtsev-Petviashvili equation in fluid dynamics, *hinese J. Phys.*, **77** (2022), 2707–2712. http://dx.doi.org/10.1016/j.cjph.2022.04.014

23. X. Gao, Y. Guo, W. Shan, Taking into consideration an extended coupled (2+1)-dimensional Burgers system in oceanography, acoustics and hydrodynamics, *Chaos Soliton. Fract.*, **161** (2022), 112293. http://dx.doi.org/10.1016/j.chaos.2022.112293

24. C. Dai, Y. Wang, Y. Fan, J. Zhang, Interactions between exotic multi-valued solitons of the (2+1)-dimensional Korteweg-de Vries equation describing shallow water wave, *Appl. Math. Model.*, **80** (2020), 506–515. http://dx.doi.org/10.1016/j.apm.2019.11.056

25. J. Fang, D. Mou, H. Zhang, Y. Wang, Discrete fractional soliton dynamics of the fractional Ablowitz-Ladik model, *Optik*, **228** (2021), 166186. http://dx.doi.org/10.1016/j.ijleo.2020.166186

26. C. Dai,Y. Fan, Y. Wang, Three-dimensional optical solitons formed by the balance between different-order nonlinearities and high-order dispersion/diffraction in parity-time symmetric potentials, *Nonlinear Dyn.*, **98** (2019), 489–499. http://dx.doi.org/10.1007/s11071-019-05206-z

27. Y. Chen, X. Xiao, Vector bright-dark one-soliton and two-soliton of the coupled NLS model with the partially nonlocal nonlinearity in BEC, *Optik*, **257** (2022), 168708. http://dx.doi.org/10.1016/j.ijleo.2022.168708

28. Q. Cao, C. Dai, Symmetric and anti-symmetric solitons of the fractional second- and third-order nonlinear Schrödinger equation, *Chinese Phys. Lett.*, **38** (2021), 090501. http://dx.doi.org/10.1088/0256-307x/38/9/090501

29. C. Dai, Y. Wang, Coupled spatial periodic waves and solitons in the photovoltaic photorefractive crystals, *Nonlinear Dyn.*, **102** (2020), 1733–1741. http://dx.doi.org/10.1007/s11071-020-05985-w

30. X. Wen, R. Feng, J. Lin, W. Liu, F. Chen, Q. Yang, Distorted light bullet in a tapered graded-index waveguide with PT symmetric potentials, *Optik*, **248** (2021), 168092. http://dx.doi.org/10.1016/j.ijleo.2021.168092
31. Y. Fang, G. Wu, X. Wen, Y. Wang, C. Dai, Predicting certain vector optical solitons via the conservation-law deep-learning method, *Opt. Laser Technol.*, **155** (2022), 108428. http://dx.doi.org/10.1016/j.optlastec.2022.108428
32. B. Li, J. Zhao, W. Liu, Analysis of interaction between two solitons based on computerized symbolic computation, *Optik*, **206** (2020), 164210. http://dx.doi.org/10.1016/j.ijleo.2020.164210
33. X. Wen, G. Wu, W. Liu, C. Dai, Dynamics of diverse data-driven solitons for the three-component coupled nonlinear Schrödinger model by the MPS-PINN method, *Nonlinear Dyn.*, **109** (2022), 3041–3050. http://dx.doi.org/10.1007/s11071-022-07583-4
34. G. Wu, L. Yu, Y. Wang, Fractional optical solitons of the space-time fractional nonlinear Schrödinger equation, *Optik*, **207** (2020), 164405. http://dx.doi.org/10.1016/j.ijleo.2020.164405
35. Z. Yan, New explicit travelling wave solutions for two new integrable coupled nonlinear evolution equations, *Phys. Lett. A*, **292** (2001), 100–106. http://dx.doi.org/10.1016/S0375-9601(01)00772-1
36. Z. Yan, Extended Jacobian elliptic function algorithm with symbolic computation to construct new doubly-periodic solutions of nonlinear differential equations, *Comput. Phys. Commun.*, **148** (2002), 30–42. http://dx.doi.org/10.1016/S0010-4655(02)00465-4
37. G. Zhang, Z. Yan, The derivative nonlinear Schrödinger equation with Zero/Nonzero boundary conditions: inverse scattering transforms and N-Double-Pole solutions, *J. Nonlinear Sci.*, **30** (2020), 3089–3127. http://dx.doi.org/10.1007/s00332-020-09645-6
38. Y. Chen, Z. Yan D. Mihalache, Soliton formation and stability under the interplay between parity-time-symmetric generalized Scarf-II potentials and Kerr nonlinearity, *Phys. Rev. E.*, **102** (2020), 012216. http://dx.doi.org/10.1103/PhysRevE.102.012216
39. X. Gao, Y. Guo, W. Shan, Bilinear forms through the binary Bell polynomials, N solitons and Bäcklund transformations of the Boussinesq-Burgers system for the shallow water waves in a lake or near an ocean beach, *Commun. Theor. Phys.*, **72** (2020), 095002. http://dx.doi.org/10.1088/1572-9494/aba23d
40. X. Gao, Y. Guo, W. Shan, T. Zhou, M. Wang, D. Yang, In the atmosphere and oceanic fluids: scaling transformations, bilinear forms, Bäcklund transformations and solitons for a generalized variable-coefficient Korteweg-de Vries-modified Korteweg-de Vries equation, *China Ocean Eng.*, **35** (2021), 518–530. http://dx.doi.org/10.1007/s13344-021-0047-7
41. B. Boubir, H. Triki, A. Wazwaz, Bright solutions of the variants of the Novikov-Veselob equation with constant and variable coefficients, *Appl. Math. Model.*, **37** (2013), 420–431. http://dx.doi.org/10.1016/j.apm.2012.03.012
42. H. Barman, A. Seadawy, M. Akbar, D. Baleanu, Competent closed form soliton solutions to the Riemann wave equation and the Novikov-Veselov equation, *Results Phys.*, **17** (2020), 103131. http://dx.doi.org/10.1016/j.rinp.2020.103131
43. R. Croke, Investigation of the Novikov-Veselov equation, an: new solutions, stability and implications for the inverse Scattering transform, Ph. D thesis, Colorado State University, 2012.

44. M. Boiti, J. Leon, M. Manna, F. Pempinelli, On the spectral transform of a Korteweg-deVries equation in two spatial dimensions, *Inverse Probl.*, **2** (1986), 271–279. http://dx.doi.org/10.1088/0266-5611/2/3/005

45. A. Kazeykina, C. Klein, Numerical study of blow-up and stability of line solitons for the Novikov-Veselov equation, *Nonlinearity*, **30** (2017), 2566.

46. B. Sagar, S. Saha, Numerical soliton solutions of fractional (2+1)-dimensional Nizhnik-Novikov-Veselov equations in nonlinear optics, *Int. J. Mod. Phys. B*, **35** (2021), 2150090. http://dx.doi.org/10.1142/S0217979221500909

47. L. Shampine, M. Reichelt, The matlab ode suite, *SIAM J. Sci. Comput.*, **18** (1997), 1–22. http://dx.doi.org/10.1137/S1064827594276424

48. P. Brown, A. Hindmarsh, L. Petzold, Using Krylov methods in the solution of large-scale differential-algebraic systems, *SIAM J. Sci. Comput.*, **15** (1994), 1467–1488. http://dx.doi.org/10.1137/0915088